Title
Nanoparticle vaccines can be designed to induce pDC support of mDCs for increased antigen display

Journal
Biomaterials Science, 11(2)

ISSN
2047-4830

Authors
Butkovich, Nina
Tucker, Jo Anne
Ramirez, Aaron
et al.

Publication Date
2023-01-17

DOI
10.1039/d2bm01132h

Peer reviewed

HHS Public Access

Author manuscript

Biomater Sci. Author manuscript; available in PMC 2024 January 09.

Published in final edited form as:

Biomater Sci. ; 11(2): 596–610. doi:10.1039/d2bm01132h.

Nanoparticle vaccines can be designed to induce pDC support of mDCs for increased antigen display

Nina Butkovich[a], **Jo Anne Tucker**[b], **Aaron Ramirez**[a], **Enya Li**[a], **Vijaykumar S. Meli**[e], **Edward L. Nelson**[b,c,d], **Szu-Wen Wang**[a,c,d,e,*]

[a]Department of Chemical and Biomolecular Engineering, University of California, Irvine, CA 92697, USA

[b]Department of Medicine, University of California, Irvine, CA 92697, USA

[c]Chao Family Comprehensive Cancer Center, University of California, Irvine, CA 92697, USA

[d]Institute for Immunology, University of California, Irvine, CA 92697, USA

[e]Department of Biomedical Engineering, University of California, Irvine, CA 92697, USA

Abstract

Cancer vaccine immunotherapy facilitates the immune system's recognition of tumor-associated antigens, and the biomolecular design of these vaccines using nanoparticles is one important approach towards obtaining strong anti-tumor responses. Following activation of dendritic cells (DCs), a robust CD8+ T cell-mediated adaptive immune response is critical for tumor elimination. While the role of efficient antigen-presenting myeloid DCs (mDCs) is conventionally attributed towards vaccine efficacy, participation by highly cytokine-producing plasmacytoid DCs (pDCs) is less understood and is often overlooked. We examined vaccines based on the E2 protein nanoparticle platform that delivered encapsulated TLR9 agonist bacterial-like DNA (CpG1826 or CpG1018) or TLR7 agonist viral ssRNA to determine their efficacy over free agonists in activating both mDCs and pDCs for antigen presentation. Although mDCs were only activated by nanoparticle-encapsulated TLR9 agonists, pDCs were activated by all the individually tested constructs, and CpG1826 was shown to induce pDC cytokine production. Transfer of secreted factors from pDCs that were stimulated with a vaccine formulation comprising peptide antigen and CpG1826 enhanced mDC display of the antigen, particularly when delivered in nanoparticles. Only when treated with nanoparticle-conjugated vaccine could pDCs secrete factors to induce antigen display on naïive mDC. These results reveal that pDCs can aid mDCs, highlighting the importance of activating both pDCs and mDCs in designing effective cancer vaccines, and demonstrate the advantage of using nanoparticle-based vaccine delivery.

*Corresponding author: wangsw@uci.edu, Phone: 949-824-2383.

5. Author contributions

Conceptualization: N.B., J.A.T., E.L.N., and S.W.W. Data curation: N.B. and J.A.T. Formal analysis: N.B. and J.A.T. Funding acquisition: E.L.N. and S.W.W. Investigation: N.B., J.A.T., A.R., E.L., and V.S.M. Methodology: N.B., J.A.T., E.L.N., and S.W.W. Project administration: E.L.N. and S.W.W. Supervision: J.A.T., E.L.N., and S.W.W. Writing – original draft: N.B., J.A.T., and S.W.W. Writing – review & editing: N.B., J.A.T., A.R., E.L., E.L.N., and S.W.W. All authors have read and agreed to the published version of the manuscript.

6. Conflicts of interest

There are no conflicts to declare.

Keywords

cancer vaccine; protein nanoparticle; myeloid dendritic cell; plasmacytoid dendritic cell; antigen display; biomaterial design

1. Introduction

Cancer is the second leading cause of death in the United States.[1] Treatment options have included surgery, chemotherapy, and radiation, which have significant side effects and have had limited efficacy.[2–4] More recently, major advances have been made in the field of cancer immunotherapy to develop cancer therapeutics, such as checkpoint inhibitors and cancer vaccines.[5–7] Cancer vaccines take advantage of the body's natural immune system to facilitate recognition of tumor-associated antigens (TAAs) and consequently induce tumor cell elimination. The design of these vaccines, which has included the use of nanoparticles functionalized with different activating elements, and understanding the mechanisms of activation by these nanomaterials, is important for promoting anti-tumor outcomes.

Dendritic cells (DCs) are a class of immune cells integral to orchestrating an anti-tumor response by cancer vaccines. A subclass of DCs, myeloid DCs (mDCs), are often implicated in efficacy due to their superior TAA display to cytotoxic T cells tasked with identifying and attacking tumor cells.[8–11] However, evidence of the importance of another subclass, plasmacytoid DCs (pDCs), has been more recently recognized but is often overlooked.[12–15] In this context, we investigated parameters to optimize nanoparticle cancer vaccine design. We hypothesized that designing protein nanoparticle cancer vaccines, which could activate pDCs in addition to mDCs, would result in enhanced vaccine efficacy.

Cancer vaccines formulated using protein nanoparticle platforms offer numerous advantages. Protein platforms are biodegradable, offer interfacial functionality, and consist of organized structures.[6] Our lab has demonstrated success using the hollow E2 caged protein as a platform for cancer vaccines (Figure 1A).[16–20] E2 is a self-assembling protein cage from the pyruvate dehydrogenase complex of *Geobacillus stearothermophilus*.[21] The E2 particle is composed of 60 identical monomers, yielding nanoparticles with diameters of ~27 nm, which mimic viruses and are optimal for uptake by antigen-presenting cells such as dendritic cells.[6, 16, 22, 23] The E2 nanoparticle can be internally and externally functionalized with non-native molecules, including Toll-like receptor (TLR) agonists and TAA, respectively.[24–29] We have shown efficacy of E2 cancer vaccines encapsulating the TLR9 agonist CpG1826 to enhance anti-tumor immunity in C57BL/6 mouse tumor models.[18–20]

We previously hypothesized that such success could be in part attributed to the exceptional ability of E2 cancer vaccines to activate mDCs,[16, 18] which are well documented in eliciting an anti-tumor response.[31–33] Namely, we predicted that E2 vaccines could be efficiently processed by mDCs, where the TLR agonist would stimulate endosomal TLRs, causing mDC activation and maturation, which we observed.[16] In these present studies, we explored the potential of E2 nanoparticles to also elicit an immune response by pDCs and whether pDC activation is important to consider in nanoparticle vaccine design.

Plasmacytoid DCs are the second major lineage of DC besides mDCs. While less abundant and less proficient at antigen presentation than mDCs, pDCs are type 1 interferon (IFN) producing cells and play a central role in responses to viral infections.[9, 34] Plasmacytoid DCs have immunomodulatory activities and can help orchestrate particular classes of systemic inflammatory responses.[8, 35–37] Activated pDCs have been shown to enhance the ability of mDCs to present TAA to T cells, increasing antigen-specific antitumor response.[13, 38] In addition to efficiently secreting type 1 IFNs, pDCs can also secrete inflammatory and Th1-skewing cytokines facilitating mDC maturation, and have the potential to transfer antigen to mDCs (Figure 1B).[14, 15] Interestingly, a recent study demonstrated that a mDC and pDC combined DC vaccine increased lymphocyte proliferation and reduced tumor volumes more than an mDC-only vaccine in a mouse lung cancer model, supporting that pDCs are important for supporting anti-tumor immunity.[13] We previously showed that E2-encapsulating TLR9 agonist could activate mDCs,[16] but if the formulations could additionally activate pDCs, and if the observation that pDCs can support mDCs holds, this could improve our mechanistic understanding of nanoparticle vaccines and help to guide the design of more effective cancer vaccines.

Stimulation of TLRs can cause the activation and maturation of mDCs and pDCs, and the choice of TLR agonist has the potential to differentially activate one or both DC types. TLR9 and TLR7 are well-conserved endosomal pattern recognition receptors that can recognize foreign genetic material. TLR9 is stimulated by bacterial-like DNA containing a non-methylated cytosine-phosphate-guanine (CpG) motif, while TLR7 is responsive to short ssRNA rich in guanosine and uridine and can include ssRNA from viruses or dead cells.[39, 40]. While murine mDCs express TLR9, murine pDCs are known to express both TLR7 and TLR9.[41, 42] We hypothesized that encapsulating adjuvants targeting different TLRs within the E2 nanoparticle could differentially activate mDCs and pDCs.

Many nanoparticle-based vaccine studies have yielded *in vivo* success by using CpG1826, a synthetic TLR9 agonist, including our own investigations where we conjugated CpG1826 to the interior of E2 nanoparticles.[18, 43–46] In these current studies, we also investigated alternative adjuvants CpG1018 and virus-derived ssRNA. While CpG1826 is a commonly used TLR9 agonist in murine studies,[6, 47, 48] CpG1018 is a TLR9 agonist included in the FDA-approved hepatitis B vaccine HEPISLAV-B®.[49, 50] Both CpG1826 and CpG1018 have sequence classified within CpG class B, the most extensively studied class of CpGs in immunology.[45, 51] The ssRNA sequence used in these studies is a TLR7 agonist derived from human immunodeficiency virus type 1 (HIV-1) long terminal repeat (nucleotides 108-127) previously shown to activate murine immune cells, including DCs.[52, 53] Each adjuvant-nanoparticle formulation, abbreviated CpG1826-E2, CpG1018-E2, and ssRNA-E2, was evaluated *in vitro*.

While recently there are increasing efforts to evaluate the beneficial role of targeting pDCs in cancer vaccines,[12] these investigations are typically not in the context of nanoparticle-based vaccines.[13, 15, 38] In this study, we therefore evaluated (1) the differential effects resulting from activation of pDC and mDCs by nanoparticle vaccines, (2) the assistance of pDC to mDCs induced by these vaccines, and (3) the potential benefits of utilizing

nanoparticle-based vaccines (Figure 1B). Thus, our investigations address the importance of a vaccine design strategy which activates both mDCs and pDCs.

2. Materials and Methods

2.1. Materials.

All buffers and reagents were purchased from Fisher Scientific, unless otherwise stated. Adjuvants CpG1826 (5'-tccatgacgttcctgacgtt-3'), CpG1018 (5'-tgactgtgaacgttcgagatga-3'), and ssRNA (5'-gcccgucuguugugugacuc-3') were custom-ordered from IDT or TriLink BioTechnologies, with or without 5' benzaldehyde modification (for nanoparticle conjugation and controls, respectively). Each DNA and RNA adjuvant included nuclease-resisting phosphorothioate (PS) backbones, especially important for protecting the ssRNA from abundant RNA-specific exonucleases *in vitro* and *in vivo*.[54] The MHC I model antigen peptide SIINFEKL ($OVA_{257-264}$) or C-SIINFEKL was synthesized by Genemed Synthesis. For DC studies, including all mDC and pDC experiments, DC culture media was comprised of RPMI 1640 (Corning), heat-inactivated fetal bovine serum (10%, Life Technologies), sodium pyruvate (1 mM, HyClone), L-glutamine (2 mM, Lonza), penicillin (100 U/mL, Gibco), streptomycin (100 μg/mL, Gibco), 2-mercaptoethanol (50 μM, Gibco), and nonessential amino acids (0.1 mM, Lonza). Recombinant human Flt3L (cross-reactive with murine receptor) was purchased from PeproTech.

2.2. E2 purification and characterization.

D381C E2 protein nanoparticles (E2) were purified and characterized as previously described.[16, 18, 24] The D381C E2 mutant has one internal cysteine modification per each of the 60 monomers, allowing conjugation of aldehyde-functionalized adjuvants in the internal hollow cavity. For purification, nanoparticle proteins were expressed in *E. coli*, and proteins in soluble lysates were separated using a HiPrep Q Sepharose anion exchange column (Cytiva) followed by a Superose 6 size exclusion column (Cytiva). For characterization, dynamic light scattering (DLS) was used to determine hydrodynamic diameters (Zetasizer Nano ZS, Malvern). Sodium dodecyl sulfate-polyacrylamide gel electrophoresis (SDS-PAGE) was used to evaluate molecular weight and purity. Proteins were stored in phosphate buffer (50 mM potassium phosphate, 100 mM NaCl, pH 7.4) at 4 °C or −80 °C for short-term or long-term storage, respectively. Residual lipopolysaccharides (LPS) were removed from E2 using Triton X-114 as previously described, confirming LPS levels of <5 EU (ng) per milligram of E2 construct using Limulus Amebocyte Lysate (LAL) assays (Genscript), levels significantly lower than necessary to activate DCs.[16] Concentrations of E2 constructs were determined using bicinchoninic acid assay (BCA).

2.3. Adjuvant and antigen conjugation to E2, and nanoparticle characterization.

Conjugation of adjuvants and peptide antigens onto E2 nanoparticles were performed using prior studies as a departure point.[16, 18] To conjugate aldehyde-modified adjuvants (Figure 2A), cysteines in the internal hollow cavity of E2 were first reduced with 10-fold excess of TCEP for at least 30 minutes. The N-(β-maleimidopropionic acid) linker was then reacted at 10-fold molar excess (relative to E2 monomer) for 2 hours at room temperature, and unreacted linker was removed with a desalting column (Zeba, ThermoFisher, 40 kDa cutoff).

A two-fold excess of aldehyde-modified adjuvant was added and incubated overnight at room temperature, with excess removed by desalting column. The conjugation ratios for each adjuvant were estimated by analyzing relative intensities of SDS-PAGE bands using NIH ImageJ software for 3 independent reactions. All reactions were conducted in phosphate buffer.

For conjugation of SIINFEKL antigen peptide on the nanoparticle surface, E2 was incubated with 20-fold excess of 4-(*N*-maleimidomethyl)-cyclohexane-1-carboxylate) (SMCC) for 30 minutes at room temperature, followed by removal of excess peptide with desalting columns. Cysteine-modified SIINFEKL (C-SIINFEKL) was reduced with 10-fold excess of TCEP for at least 30 minutes, then incubated with the E2 sample. Excess peptide was removed with desalting columns. Mass spectrometry (Xevo QTof) was used to quantify the number of SIINFEKL peptides conjugated per E2 nanoparticle.[16] All E2 constructs were characterized with BCA, DLS, and SDS-PAGE, as previously described.[16, 18] For transmission electron microscopy (TEM), protein samples were stained with 2% uranyl acetate on carbon-coated copper grids (Ted Pella) and imaged using a JEM-2100F electron microscope.

2.4. Bone marrow (BM)-derived mDC and pDC differentiation.

Studies requiring animals were carried out according to protocols approved by the Institute for Animal Care and Use Committee (IACUC) at the University of California, Irvine. For all experiments, C57BL/6 female mice purchased from Jackson Laboratories were used from 6-12 weeks of age. Murine BM-derived mDCs and pDCs were cultured *in vitro* following previously published protocol[16, 36] as outlined in Figure SI-1, prior to incubation with E2 nanoparticles or controls. Briefly, femurs and tibias from 6- to 12-week-old mice were harvested and washed with 70% ethanol. BM was flushed with sterile PBS (137 mM NaCl, 2.7 mM KCl, 10 mM disodium phosphate, 1.8 mM potassium phosphate; Gibco) and centrifuged at 300 x g for 5 min, with supernatant discarded. Red blood cells were depleted with re-suspension ACK lysing buffer (Lonza) for 2 minutes, followed by washing with PBS.

Cells were maintained at 37 °C and 5% CO_2. For mDCs, BM cells were plated at 2 x 10^5 cell/mL (10 mL total) into sterile bacteriological non-tissue-culture treated Petri dishes in DC media with murine recombinant GM-CSF (20 ng/mL). Fresh media with growth factor was replaced on Day 3 and Day 6. On Day 7, non-adherent mDCs were collected and seeded into 48-well plates (Corning Falcon) at a density of 200,000 cells/well (500 μL per well) and allowed to settle overnight. For pDCs, BM cells were seeded at 1 x 10^6 cells/mL (5 mL per well) into 6-well tissue culture plates (Costar) on Day 0 and cultured for one week in DC media with Flt3L (200 ng/mL, PeproTech) without media change.

2.5. Activation and analysis of mDCs or pDCs.

Protocols for DC activation studies following differentiation are outlined in Figure SI-1. Myeloid DCs were incubated with the test groups PBS, 100 ng/mL LPS (eBioscience), E2 nanoparticle alone, free adjuvant, or adjuvants attached to E2 (E2-adjuvant) for a range of concentrations for 24 hr starting on Day 8. On Day 9, cells were collected after washing with PBS and stained with anti-CD11c (FITC), -MHC II (PE/Cy7), and -CD86 (APC) mouse

antibodies (eBioScience, BioLegend) for analysis with flow cytometry (ACEA Novocyte, FlowJo).

Plasmacytoid DCs were incubated with the test groups PBS, 200 ng/mL LPS, E2 nanoparticle, free adjuvant, or adjuvants attached to E2 (adjuvant-E2) for a range of concentrations for 24 hr starting on Day 8. On Day 9, cells were collected after washing with PBS and stained with anti-CD11c (FITC), -B220 (APC/Cy7), -MHC II (PE/Cy7), and -CD86 (APC) mouse antibodies (BioLegend) for analysis with flow cytometry (ACEA Novocyte, FlowJo). For viability studies, monocytes were differentiated into pDCs as described above through Day 7, then incubated with PBS, CpG1826, or CpG1826-E2 for 24 hr starting on Day 8. On Day 9, cells were collected after washing with PBS as outlined in Figure SI-2A. As a positive control to identify dead cells, samples were heat shocked to 60 °C for 10 min to induce cell death, while cells incubated with PBS alone served as the control for live cells. All samples were stained using the LIVE/DEAD™ Fixable Aqua Dead Cell Stain Kit (Invitrogen) according to the instructions with a 2:1000 ratio between reconstituted dye and PBS, followed by staining with anti-CD11c (FITC) and -B220 (APC/Cy7) mouse antibodies (BioLegend) for analysis with flow cytometry (ACEA Novocyte, FlowJo).

2.6. SIINFEKL display by mDCs or pDCs, and studies assessing pDC support of mDCs.

Myeloid and plasmacytoid DCs were differentiated as described above. To assess antigen display by mDCs or pDCs without media transfer (Figure SI-3), mDCs and pDCs were then incubated with the test groups PBS, 2 μg/mL SIINFEKL (positive control), 0.1 μg/mL free CpG1826 with 0.1 μg/mL free SIINFEKL (CpG + S), or 1 μg/mL CpG-S-E2 (CpG1826 and SIINFEKL attached to nanoparticle) using the following schedules. Myeloid DCs were incubated for 24 hr starting on Day 9 or Day 10. Plasmacytoid DCs were gently washed with DC media three times, the media was replaced, and the cells were then incubated with condition for 24 hr or 48 hr starting on Day 8. After incubation period, mDCs were stained with anti-CD11c (FITC) and -H-2Kb bound to SIINFEKL (APC) mouse antibodies, while pDCs were stained with anti-CD11c (FITC), -B220 (APC/Cy7), and -H-2Kb bound to SIINFEKL mouse antibodies (BioLegend, eBioscience).

To investigate the effects of pDC assistance on mDC antigen display (studies investigating pDC support of mDCs), we cultured pDCs with the nanoparticles or controls, collected the media, and cultured mDCs in this transferred media. Myeloid and plasmacytoid DCs were differentiated in parallel from the same mouse, with GM-CSF or Flt3L (respectively) for one week, as described above. On Day 8, pDCs were incubated with 1 μg/mL CpG-S-E2 or controls (PBS or 0.1 μg/mL free CpG1826 with 0.1 μg/mL free SIINFEKEL) for 4 hr followed by gentle washing with media three times and replacement of media volume. On Day 9 or Day 10 (after 24 hr or 48 hr incubation, respectively), pDC media was collected. This culturing period was consistent with that used in other studies.[15] For media transfer, 80% of mDC media per well was removed (from 48-well plates) and replaced with media collected from the pDC cultures. As a control group, some mDCs were maintained in the full volume of their original media. All mDCs were then incubated with PBS, 2 μg/mL SIINFEKL (positive control), 0.1 μg/mL free CpG1826 with 0.1 μg/mL free SIINFEKEL, or

1 μg/mL CpG-S-E2 for 24 hr. The following day, mDCs were collected after washing wells with PBS and analyzed with flow cytometry as performed in the antigen display studies.

To analyze cytokines expressed by pDC in the media after incubation, 24 hr and 48 hr incubation samples were collected. Murine Mix and Match LEGENDPlex™ assay (BioLegend) was utilized as recommended by the manufacturer, with final samples analyzed using flow cytometry (Novocyte, FlowJo). Analyzed cytokines included murine tumor necrosis factor alpha (TNF-α), interleukin-12p70 (IL-12p70), interleukin-10 (IL-10), interleukin-6 (IL-6), and interferon-beta (IFN-β).

2.7. Statistical analyses.

Statistical analyses were performed using GraphPad Prism8. For particle characterization, mean ± standard deviation was calculated for 3 independent conjugation batches. In all plots of *in vitro* DC data, mean ± SEM of n ≥ 3 independent biological replicates are displayed, with ≥ 2 technical replicates for each biological replicate. Statistical significance was analyzed by one-way analysis of variance (ANOVA) followed by Bonferroni post-tests. For activation studies, each dosage of adjuvant-E2 was compared to PBS or the equivalent dosage of E2 or free adjuvant. In antigen display studies, incubation with PBS or free CpG1826 with free SIINFEKL was compared to incubation with CpG-S-E2. To compare mDC antigen display with (+) or without (−) pDC supernatant transfer, +/− media transfer conditions were compared to each other, and data correlating to mDCs incubated with PBS was compared to other incubation conditions. For cytokine analysis, all incubation conditions per incubation time per cytokine were compared.

3. Results & Discussion

3.1. Conjugation of adjuvants and peptide antigen to E2 yielded intact nanoparticles

TLR agonists CpG1826, CpG1018, and ssRNA were successfully encapsulated within the internal hollow cavity of E2 nanoparticles at relatively high packing efficiencies. The results of these adjuvant conjugations are shown in Figure 2. After conjugating each adjuvant individually to the interior of E2 (Figure 2A), we characterized nanoparticles using numerous techniques. SDS-PAGE characterization (Figure 2B) showed a single unconjugated E2 monomer in lane 2 (theoretical molecular weight 28.1 kDa, control) and 2 bands each for CpG1826-E2, CpG1018-E2, and ssRNA-E2 in lanes 3-5 – one corresponding to the E2 monomer (28.1 kDa) and the other to adjuvant-conjugated E2 monomer (34.9 kDa, 35.7 kDa, and 35.1 kDa, respectively). CpG conjugations were confirmed by mass spectrometry (Figure SI-4). All measured masses were within 1 Da of the theoretical value, with E2, BMPH-E2, CpG1826-E2, and CpG1018-E2 corresponding to 28105 Da, 28287 Da, 34878 Da, and 35666 Da, respectively.

We determined the number of adjuvant molecules conjugated to each E2 nanoparticle to be 21.5 ± 2.7 CpG1826, 20.2 ± 3.2 CpG1018, and 25.6 ± 2.7 ssRNA, corresponding to approximately 35%-40% of the theoretical maximum of 60. Thus for each conjugate, approximately 0.1 μg of adjuvant was encapsulated per of 1 μg of construct, consistent with previously reported attachment yields of CpG1826 following the same attachment

approach.[16] Since the lengths of each genetic sequence are nearly the same (~20 nucleotides), similar packing efficiencies for each adjuvant were expected.

All adjuvant-encapsulated constructs maintained uniform nanoparticle size and structure. DLS measured hydrodynamic diameters of ~27 nm (Figure 2C), which is within the optimal particle size range for DC uptake.[22, 23] Diameters averaged 27.1 ± 1.1 nm (E2); 27.0 ± 1.4 nm (CpG1826-E2); 26.6 ± 1.7 nm (CpG1018-E2); and 28.0 ± 1.2 nm (ssRNA-E2). TEM confirmed intact particles corresponding to this size as well, with consistent shape and size independent of conjugated adjuvant (Figure 2D). With these E2 nanoparticles encapsulating TLR7 or TLR9 agonist, we could assess differential activation of mDCs and pDCs.

While E2 encapsulating TLR agonist is necessary for DC activation, the conjugation of antigen on E2 nanoparticles is required for eliciting a targeted immune response and assessing antigen display by DCs. To investigate the role of mDCs and pDCs in antigen processing and display, nanoparticles conjugated with the model epitope SIINFEKL (from ovalbumin) were made. We conjugated CpG1826-SIINFEKL-E2 (abbreviated as CpG-S-E2) as previously described (Figure 2A,E) and characterized nanoparticles.[16] The conjugation of C-SIINFEKL with linker on the surface of the nanoparticle was predicted to increase the E2 monomer molecular weight by 1.3 kDa per peptide that is conjugated, and the conjugation of multiple peptides resulted in wide bands on SDS-PAGE corresponding to CpG-S-E2 and SIINFEKL-E2 (abbreviated S-E2) (Figure 2F). Peptide conjugation ratios and SDS-PAGE characterization were consistent with previously reported data, with 2.9 ± 0.3 peptides conjugated per monomer (i.e., ~174 peptides per 60-mer nanoparticle), or approximately 0.1 μg of peptide displayed per 1 μg E2 construct.[16] DLS confirmed that nanoparticles remained intact, with E2 and CpG-S-E2 yielding diameters of 27.1 ± 1.1 nm and 29.1 ± 2.9 nm, respectively, consistent with previously reported values (Figure 2G).[16]

3.2. Myeloid and plasmacytoid DCs were differentially activated by encapsulated TLR agonists

3.2.1. Characterization of mDCs and pDCs.—We hypothesized that mDCs and pDCs are both critical for eliciting an optimal anti-tumor response following vaccination (Figure 1B). While mDCs are superior antigen-displaying cells, pDCs are more efficient at secreting pro-inflammatory cytokines and type I interferons (IFNs) than mDCs, producing 10^2 to 10^3 times more type I IFNs than any other cell.[55, 56] Therefore, pDCs can assist in the activation of mDCs, but aid of pDCs by mDCs is, by contrast, less likely.

In order to study the interaction of these populations, bone marrow (BM) cells were induced to differentiate into mDCs and pDCs *in vitro*. For differentiation, we harvested murine BM, depleted red blood cells, and incubated cells with growth factor (GM-CSF for mDC or Flt3L for pDC differentiation) over the course of one week.[36, 56] Appropriate phenotype for each population was confirmed by CD11c and B220 expression as previously described; mDCs were gated as $CD11c^{high}$ and $B220^{-}$ (Figure 3A), and pDCs were gated as $CD11c^{low}$ and $B220^{+}$ (Figure 3B).[36] Our recovery and observed populations were consistent with previous reports.[38, 57] In mDC cultures, a second population was observed comprising smaller cell sizes (Figure 3A), similar to those in the pDC population (Figure 3B). However, these cells were $CD11c^{-/low}B220^{-}$ and therefore did not exhibit pDC or mDC phenotype;

thus, cells in this population were not included in the analyses. It should be noted that generating pDCs with Flt3L can tend to cause a non-uniform expression of CD11c or B220, though we confirmed that the majority of cells (approximately 60% of cells) exhibited a pDC phenotype (Figure 3B).[36, 56] Induced mDC and pDC populations were necessary for this study due to the scarcity of *ex vivo* isolated cells; the efficient yields and largely faithful phenotype resulting from differentiation with GM-CSF or Flt3L supports *in vitro* differentiation as a powerful tool for modeling *in vivo* DC populations.[58]

3.2.2. Myeloid DCs are activated by nanoparticle-encapsulated TLR9 agonist, but not TLR7 agonist.—For activation studies, differentiated mDCs and pDCs were incubated with E2 encapsulating CpG1826, CpG1018, ssRNA, or with controls (PBS, LPS, or free adjuvant) as outlined in Figure SI-1. It is documented that pDCs and mDCs can be activated with LPS and thus, LPS was chosen as the positive control.[59] The expression of mDC activation markers MHC II (Figure 4A–C) and CD86 (Figure SI-5A–C) followed similar trends. Similarly, pDC expression of MHC II (Figure 4D–F) and CD86 (Figure SI-5D–F) were consistent. The upregulation of MHC II and CD86 are necessary for T cell activation and are indicators for the activation of mDCs or pDCs.[57, 60] Our results show that the encapsulation of either CpG1826 or CpG1018 in E2 nanoparticles increased mDC activation over free adjuvant alone, approximately doubling MHC II or CD86 MFI (relative to PBS), comparable to LPS stimulation; however, no significant increase was observed following mDC incubation with either free or E2-encapsulated ssRNA at the comparable conditions tested.

In comparing the TLR9-induced activation of mDCs, we observe that CpG1826-E2 and CpG1018-E2 increased activation marker levels to similar extents. Both MHC II and CD86 marker expressions increased after incubation with CpG1826-E2, at concentrations of 5 μg/mL to 10 μg/mL or 30 μg/mL CpG1826-E2 (Figure 4A; Figure SI-5A). In contrast, free CpG1826 or E2 at equivalent dosages did not cause mDC activation. Encapsulating CpG1018 in E2 similarly improved mDC activation compared to free CpG1018, approximately increasing MHC II or CD86 MFI 2- to 3-fold versus PBS (Figure 4B; Figure SI-5B). These results show that CpG-based TLR9 agonists encapsulated within the nanoparticle increased mDC activation, while free TLR9 agonist tended to activate minimally or not at all under the same concentrations.

As expected and in contrast to CpG results, free or encapsulated ssRNA did not increase mDC MHC II or CD86 expression at any tested concentration (Figure 4C; Figure SI-5C). There is some conflict in the literature as to the mDC response to TLR7 ligands. Although some studies report mDC activation by TLR7 ligands,[61–63] others show that TLR7 expression is subset-dependent and that mDC activation by these ligands may occur through other signaling pathways.[42, 64–66]

3.2.3 Plasmacytoid DCs are activated by nanoparticle-encapsulated TLR9 and TLR7 agonists.—Plasmacytoid DCs were activated by both nanoparticle-delivered and free TLR9 agonist. As the dosage was increased from 0.2 μg/mL to 5 μg/mL of CpG1826-E2 or CpG1018-E2 constructs, pDC activation marker expressions increased, approximately doubling the MFI versus PBS (Figure 4D,E; Figure SI-5D,E). Both 1 μg/mL

and 5 μg/mL of either construct with either TLR9 agonist increased MHC II or CD86 expression levels, relative to PBS or E2 negative controls.

Unlike mDCs, TLR9 agonists in pDCs did not need to be delivered in a nanoparticle to elicit an increase in activation marker expression, with optimal adjuvant concentrations around 0.1 μg/mL CpG1826 or 0.5 μg/mL CpG1018. Plasmacytoid DC activation marker levels peaked at a concentration of 0.1 μg/mL free CpG1826, then decreasing as concentration increased to 0.5 μg/mL free CpG1826 (Figure 4D; Figure SI-5D). We speculated that this observation is likely due to over-activation leading to cell death or anergy.[67, 68] To examine this, we subsequently assessed pDC cell viability following stimulation with free or E2-encapsulated CpG1826 at equivalent concentrations and confirmed that regardless of incubation condition, pDCs maintained high viability at around 90% (Figure SI-2B). Therefore, it is more likely that the decrease in activation marker expression at high free CpG1826 concentrations is due to the pDCs exhibiting anergic behavior rather than toxicity of the agonist. This response is consistent with observations by Volpi *et al.*, who demonstrated that a ten-fold increase in CpG1826 administered to murine pDCs can induce a tolerogenic phenotype.[68]

We note that this decrease in pDC activation marker expression at higher free CpG1826 concentrations is not observed in the equivalent amount of E2-encapsulated CpG. We may be observing an additional benefit of adjuvant encapsulation, presumably due to the kinetics of nanoparticle processing. Namely, CpG1826-E2 containing 0.5 μg/mL CpG1826 maintained robust activation levels compared to 0.5 μg/mL free CpG1826, suggesting that with encapsulation, the pDC dose response may be shifted, potentially preventing anergy at this CpG1826 concentration.

Unlike in mDCs, nanoparticle encapsulation of the ssRNA caused activation of pDCs. MHC II and CD86 expressions increased from 0.2 μg/mL to 5 μg/mL of E2-ssRNA construct in a dosage-dependent manner, approximately doubling MFI versus PBS (Figure 4F; Figure SI-5F). However, the equivalent concentrations of free ssRNA failed to cause activation. Plasmacytoid DCs are integral for mounting anti-viral immunity and express higher levels of TLR7 than mDCs, so activation with encapsulated ssRNA in a virus-like particle is not unexpected.[41, 42, 69, 70]

3.2.4. Encapsulation of adjuvants in nanoparticles.—There are numerous advantages to encapsulating adjuvant within a nanoparticle vaccine formulation versus the application of free adjuvant. Previous studies revealed that encapsulating CpG1826 adjuvant within E2 nanoparticles enhanced mDC activation *in vitro*, suggesting more efficient uptake and cellular trafficking to allow the TLR9 agonist to interact with TLR9 in the endosomal compartment than free TLR9 agonist.[16, 18] The ~27 nm E2 nanoparticle vaccines can efficiently deliver adjuvant and antigen to DCs simultaneously. This is advantageous for eliciting a specific immune response following endosomal processing, a phenomenon observable for other particle systems as well.[44, 71] Furthermore, encapsulation of nucleotides within a nanoparticle may shield these adjuvants from nucleases, providing an additional form of protection besides the use of a PS backbone. Compared to CpGs, ssRNA is especially susceptible to nuclease degradation, even with phosphodiester linkages.[72, 73] Our

observed data showing activation of pDCs by encapsulated (but not free) TLR7 agonist could be explained by enhanced protection of the cargo from the variety of nucleases in this model system. We observed benefits of DNA or RNA delivery within a nanoparticle for both mDCs and pDCs, leading to increased activation.

Plasmacytoid DCs have been shown to be highly sensitive to TLR9 and TLR7 agonists, supporting their critical role in mounting rapid inflammatory cytokine response against invading pathogens.[74, 75] In contrast, studies have shown that mDCs are robustly activated by TLR9 agonists, but the lack of TLR7 in a significant portion of the cell population can hinder response to TLR7 agonists.[41, 42] The differential activation we observed by E2-encapsulated TLR agonists is consistent with TLR expression levels reported in the literature.[42, 74] To further investigate the pDC response induced by nanoparticles encapsulating TLR9 agonist, we assessed their cytokine production after incubation with vaccine formulations.

3.3. Plasmacytoid DCs secrete an array of pro-inflammatory cytokines in response to stimulation with CpG-S-E2 nanoparticles

Plasmacytoid DCs are known for secreting significantly higher amount of cytokines, such as type I IFNs, compared to mDCs.[34] In the case of autoimmune diseases such as psoriasis or systemic lupus erythematosus, pDCs can exacerbate symptoms by secreting high levels of type I IFNs following TLR stimulation.[34, 69] However, the same cytokine production framework can be highly beneficial in promoting anti-viral, -bacterial, and -cancer innate and adaptive immune responses.[76, 77] Therefore, it would be desirable for nanoparticle vaccines to elicit pro-inflammatory cytokine production from pDCs. We are not aware of other studies which have demonstrated that nanoparticles encapsulating adjuvant can initiate a cytokine production response by pDCs.

To perform these studies, we formulated CpG-S-E2, nanoparticles containing CpG1826 (abbreviated CpG) and displaying SIINFEKL antigen (abbreviated S). Plasmacytoid DCs were incubated with CpG-S-E2 nanoparticles (or free CpG with SIINFEKL antigen) for 24 hr or 48 hr (after a 4-hr incubation and a washing step), and secreted cytokines were analyzed (Figure 5). After 24 hr incubation, pDCs that had been incubated with nanoparticle vaccine secreted highest levels of IFN-β (Figure 5A), TNF-α (Figure 5B), IL-6 (Figure 5C), IL-10 (Figure 5D), and IL-12p70 (Figure 5E) approximately two-fold or more over PBS. By contrast, stimulation with 0.1 μg/mL free CpG1826 with 0.1 μg/mL free SIINFEKL (abbreviated as CpG + S) at an equivalent adjuvant and antigen dosage did not significantly increase cytokine secretion over PBS, suggesting altered kinetics of activation and cytokine secretion previously observed in pDCs.[78]

Each of these cytokines is known to modulate the activity of immune cells, including mDCs, as elaborated below. For either timeline, pDCs stimulated with CpG-S-E2 generated robust IFN-β (Figure 5A), TNF-α (Figure 5B), and IL-6 (Figure 5C) levels. IFN-β, TNF-α, and IL-6 are pro-inflammatory cytokines which pDCs can efficiently secrete, fostering inflammatory responses.[76, 79] For instance, TNF-α can induce direct cell killing of tumors and enhance immune cell activation.[79] While IL-10 (Figure 5D) and IL-12p70 (Figure 5E) secretion was increased following vaccine stimulation for the 24 hr incubation, levels

decreased approximately 4-fold after 48 hr incubation. IL-10 can act as an anti-inflammatory cytokine whose secretion can inhibit IL-12p70 secretion and pDC activation, though under certain circumstances IL-10 can promote the proliferation of cytotoxic T cells.[80, 81] IL-12p70 is Th1-skewing, inducing naïive T helper cells to differentiate into Th1 cells, important for antitumor response.[82] Higher IL-10 concentration for pDCs stimulated with vaccine and incubated 24 hr could be one reason IL-12p70 concentration after 48 hr was greatly diminished, though the exact mechanism is well beyond the scope of this report.

The secretion of cytokines is a highly dynamic process dependent on several variables, including the kinetics of intracellular machinery, uptake of cytokines by cells, and even cytokine degradation. Taken altogether, these results indicate that the nanoparticle vaccine with encapsulated CpGs can activate pDCs and robustly trigger a pro-inflammatory, Th1-skewed response. Given this observation, we predicted that conditioned media from E2 vaccine-stimulated pDCs could facilitate mDC antigen presentation capabilities (Figure 1B). Therefore, we next investigated antigen display of mDCs and pDCs individually and together in a cooperative model for pDC support of mDCs after incubation with CpG-S-E2.

3.4. Both mDCs and pDCs can display model antigen epitopes delivered on E2 nanoparticles

Before examining the assistance of pDC to mDC in antigen display, we first selected the optimal concentration of adjuvant for each. From the mDC and pDC activation studies, 1 μg/mL CpG1826-E2 nanoparticles activated pDCs (Figure 4D; Figure SI-5D), but the equivalent dosage in mDCs was projected to elicit minimal or no activation, based on shifts in MHC II and CD86 marker expression (Figure 4A; Figure SI-5A). Therefore, for antigen display studies, pDCs and mDCs were incubated with 1 μg/mL CpG-S-E2 vaccine formulation (containing 0.1 μg/mL each of CpG1826 and SIINFEKL) or controls (PBS or CpG + S) using the protocols outlined in Figure SI-3.

Myeloid DCs displayed SIINFEKL peptide on MHC I after incubation with CpG-S-E2 nanoparticles (containing CpG1826 and SIINFEKL) for 24 hr (Figure SI-6A,B). For pDCs, incubation with CpG-S-E2 slightly increased average antigen display over incubation with PBS or CpG + S (at equivalent CpG and antigen concentrations) but this was not statistically significant (Figure SI-6C). However, antigen display increased after 48-hr incubation and was indeed significant; the antigen display was approximately 1.5 times higher for the nanoparticle group than display following incubation with CpG + S control (Figure SI-6D). Although free CpG1826 and CpG1826-E2 activated pDCs in a similar dose-dependent manner (Figure 4D, Figure SI-5D), the co-delivery of both CpG and antigen peptide on the E2 scaffold appears to more efficiently facilitate pDC antigen display.

3.5. Plasmacytoid DCs can aid the display of antigen by mDCs and do so more effectively via nanoparticle-based delivery of antigen and adjuvant, demonstrating the importance of nanoparticle vaccine design

To investigate our hypothesis that the engagement of both mDCs and pDCs could result in improved anti-tumor responses, we investigated cooperation studies involving pDC secreted factors supporting mDCs. We used an *in vitro* experimental protocol to examine this

support (Figure 6A). The *in vitro* support model used in this study models the *in vivo* microenvironment in the spleen and other secondary lymphoid organs, which can house activated pDCs and mDCs in the same anatomic compartment, and has been validated in a previous study.[12, 15] Importantly, the concentration of CpG-S-E2 used for stimulating mDCs was below the threshold for eliciting activation and antigen display. The wash steps described were important to help minimize the transfer of residual vaccine and/or adjuvant and antigen from pDC wells to mDCs; media transferred from pDCs to mDCs could be presumed to contain factors secreted by pDCs, potentially including cytokines and antigens in some form,[15, 34] but minimal to no carry-over vaccine or CpG with peptide dosage. With pDC incubation periods of 24 hr (Figure 6B–E) or 48 hr (Figure SI-7), we saw similar trends.

Experiments confirmed that transferring conditioned media from non-stimulated pDCs to mDCs did not alter mDC antigen display capabilities. Regardless of the timeline tested (24 hr or 48 hr) and mDC treatment condition after media transfer, media transferred from non-stimulated pDCs (pDCs incubated with PBS) did not alter mDC peptide display (Figure 6B; Figure SI-7A). Based on these control experiment results, non-stimulated pDCs did not release sufficient secreted factors to aid mDCs in displaying antigen more efficiently. Notably, transferring media from pDCs incubated with PBS demonstrated that the CpG-S-E2 concentration incubated with mDCs, in and of itself, was insufficient to elicit an elevated amount of antigen display over the no-transfer condition (Figure 6B).

We observed that transfer of media from pDCs incubated with adjuvant and antigen, in the form of CpG + S (free molecules) or CpG-S-E2 (nanoparticle), could aid mDC antigen display. Media was collected from pDCs treated with PBS, CpG + S, or CpG-S-E2. Resulting 24 hr (Figure 6C–E) or 48 hr (Figure SI-7B–D) conditioned pDC media was transferred to mDCs, and then mDCs were treated with PBS, CpG + S, or CpG-S-E2 for 24 hr. Interestingly, mDCs demonstrated antigen presentation capacity even if they were never directly incubated with any antigen themselves (Figure 6C). If pDCs were incubated with the CpG-S-E2 nanoparticle, the resulting conditioned media from pDCs aided mDCs (which had been incubated only with PBS prior to the media transfer) to display SIINFEKL (Figure 6C). These data support that conditioned media included secreted cytokines and antigen in some formulation, which can result in antigen display by mDCs. These results also show the advantage of delivering CpG and peptide together in the context of a nanoparticle (versus free in solution) since media from pDCs that were treated with free CpG + S did not result in display of the SIINFEKL peptide by the mDCs. Nanoparticle formulations may have resulted in more efficient pDC antigen processing and secretion of exosomes or other antigen containing structure and enhanced cytokine secretion,[34, 83] the latter of which we observed by ELISA analysis (Figure 5).

Similar trends were observed when mDCs were incubated with conditioned media from pDCs and also with CpG + S (Figure 6D). It is notable that mDCs had a very low or no level of activation and antigen display when incubated with CpG + S (Figure 4A; Figure 6B,D). However, when mDCs were incubated with conditioned media from pDCs in CpG-S-E2 (or CpG + S) together with the CpG-S-E2 nanoparticle, there was increased mDC antigen display (Figure 6D,E) despite having concentrations of CpG-S-E2 that were

below the threshold for mDC activation. Myeloid DCs had statistically similar levels of antigen display when conditioned media was transferred from pDCs incubated with 0.1 μg/mL SIINFEKL instead of 0.1 μg/mL CpG with 0.1 μg/mL SIINFEKL, regardless of mDC incubation condition (data not shown). Similar results were observed when pDCs were cultured for 48 hr instead of 24 hr following wash steps (Figure SI-7B–D). We note that regardless of the mDC incubation condition following media transfer, conditioned media from pDCs incubated with the nanoparticles (CpG-S-E2) enhanced mDC antigen display, demonstrating the importance of the nanoparticle in adjuvant and antigen delivery and showing an advantage to delivery of adjuvant and antigen attached to a nanoparticle.

These results support that the efficacy of the E2 nanoparticle-based vaccine encapsulating CpG1826, which we had previously observed *in vivo*.[18,20] This efficacy may be due, in part, to its ability to activate both mDCs and pDCs and elicit cytokine production in pDCs.[14, 15] Because both murine mDCs and pDCs express TLR9 and are predicted to have responded to our nanoparticle vaccine, based on our data, it is likely that pDCs play a significant role in the observed efficacy of nanoparticle anti-tumor vaccines *in vivo*.[6, 41, 42] Numerous preclinical murine studies have validated the use of CpGs in cancer vaccines to support anti-tumor immunity, triggering tumor-specific cytotoxic T cell proliferation and tumor volume reduction.[18, 46, 84] The use of TLR7 agonist in cancer vaccine development has also been studied, though perhaps less extensively.[45, 85] Formulations using TLR7 agonist have been shown to have potential to increase antigen-specific CD8+ T cell and pDC activation *in vivo*, consistent with our observed responsiveness of murine pDCs to TLR7 agonist.[86, 87] Overall, our results here support that selecting CpG as an adjuvant in cancer vaccines can lead to a robust anti-tumor response in murine tumor models, in part by eliciting support by pDCs to mDCs in antigen display.

4. Conclusions

In these studies, we designed immune-activating protein nanoparticles and demonstrated their ability to activate two major DC subsets *in vitro*. E2 nanoparticles were conjugated to ligands that are agonists for different TLRs,[88] including CpGs and ssRNA, which stimulate TLR9 and TLR7, respectively. All constructs maintained optimal size for uptake by DCs,[22] and similar attachment yields were observed for each adjuvant. To investigate the response of DC subsets induced by E2 encapsulating TLR agonist, murine mDCs and pDCs were differentiated *in vitro* and exhibited expected characteristics of each population.

Both DC populations could uptake and process the nanoparticles, leading to endosomal TLR stimulation and model antigen display. Depending on the conjugated adjuvant, E2 nanoparticles were shown to differentially activate the two main DC lineages. E2 encapsulating CpGs robustly activated mDCs, critical for antigen display to T cells and formerly believed to be the primary mode of eliciting immune response in murine experiments. E2 containing CpGs or ssRNA stimulated pDCs, a less abundant DC subset known to efficiently and robustly secrete pro-inflammatory, Th1-skewing cytokines in response to viral infections, but less studied in the field of cancer vaccines. Differential activation of mDCs and pDCs by ssRNA-E2 is due to higher levels of TLR7 expression in murine pDCs. This is the first study demonstrating the potential of E2 nanoparticle

encapsulating TLR9 agonist to activate both murine mDCs and pDCs. As DC activation is dependent on TLR content, the specific responses observed here are likely dependent on the animal model used; for instance, mouse and human DCs express different endosomal TLRs.[41, 42, 89] However, these studies more broadly suggest that protein nanoparticle vaccines should be formulated to specifically activate both major mammalian DC subsets.

The results of the pDC-mDC support study suggest that pDCs incubated with the E2 vaccine demonstrate a robust ability to secrete factors, which aid mDC antigen display. Our investigation of pDC support of mDCs in antigen presentation suggests a potential mechanism by which E2-based vaccines stimulate a very effective anti-tumor immune response *in vivo*. Our studies are in support of previous literature that demonstrated pDC secretion of exosomes containing antigen,[15] as we observed that mDCs incubated with PBS (and no antigen) were able to present antigen if given conditioned media from pDCs stimulated with the nanoparticle vaccine (CpG-S-E2). The analysis of pDC cytokine secretion after stimulation with vaccine also strongly suggests that an array of pro-inflammatory cytokines may facilitate mDC activation and antigen display. Since mDCs are superior to pDCs at presenting antigen,[8] the aid of mDCs by pDCs may be an evolved mechanism to enhance systemic immune response against viruses and virus-like particles. Our demonstration of pDC support of mDCs in antigen presentation suggests a potential mechanism by which E2-based vaccines stimulate a very effective immune response *in vivo* and may explain the potency of nanoparticle-based vaccines in treating infectious diseases and cancer.[47] Taken altogether, these studies suggest it would be advantageous for cancer vaccine therapies that target DCs to be designed to activate both mDCs and pDCs and that delivering adjuvant and antigen in nanoparticle formulation is highly beneficial over a conventional mixture of adjuvant and antigen.

Supplementary Material

Refer to Web version on PubMed Central for supplementary material.

Acknowledgements

This work was supported by the National Institute of Biomedical Imaging and Bioengineering (R01EB027797) and the National Cancer Institute (P30CA062203) of the National Institutes of Health. The content is solely the responsibility of the authors and does not necessarily represent the official views of the NIH. Flow cytometry, mass spectrometry, and TEM were carried out at the UCI Institute for Immunology Flow Cytometry Facility, UCI Mass Spectrometry Facility, and UCI TEM Facility in IMRI, respectively. We would like to thank Dr. Li Xing for TEM training; Dr. Benjamin Katz and Dr. Felix Grun for mass spectrometry training; the Cancer Center Support Grant (CCSG) and Shared Resources for help with statistical analysis; and Andrew Rowley for helpful discussions. Portions of Figures 1, SI-1, SI-2, SI-3, and 6 were generated using BioRender. Molecular graphics were created using ChimeraX, developed by the Resource for Biocomputing, Visualization, and Informatics at the University of California, San Francisco, with support from the National Institute of Health (R01GM129325) and the Office of Cyber Infrastructure and Computational Biology, National Institute of Allergy and Infectious Diseases.

Abbreviations:

BM	bone marrow
CpG	cytosine-phosphate-guanine
DC	dendritic cell

DLS	dynamic light scattering
E2	protein nanoparticle derived from the E2 subunit of pyruvate dehydrogenase (D381C form of E2 was used in this study)
IFN	interferon
IL	interleukin
LPS	lipopolysaccharides
mDCs	myeloid dendritic cells
pDCs	plasmacytoid DCs
PS	phosphorothioate
SDS-PAGE	sodium dodecyl sulfate-polyacrylamide gel electrophoresis
TAA	tumor associated antigen
TEM	transmission electron microscopy
TLR	Toll-like receptor
TNF	tumor necrosis factor

6. References

1. Richardson L, Dowling N and Henley J, An Update on Cancer Deaths in the United States, https://www.cdc.gov/cancer/dcpc/research/update-on-cancer-deaths/index.htm, (accessed April, 2022).
2. Baskar R, Lee KA, Yeo R and Yeoh KW, Int J Med Sci, 2012, 9, 193–199. [PubMed: 22408567]
3. Albano D, Benenati M, Bruno A, Bruno F, Calandri M, Caruso D, Cozzi D, De Robertis R, Gentili F, Grazzini I, Micci G, Palmisano A, Pessina C, Scalise P, Vernuccio F, Barile A, Miele V, Grassi R, Messina C and Young SWG, Insights Imaging, 2021, 12, 76. [PubMed: 34114094]
4. Hanna TP, King WD, Thibodeau S, Jalink M, Paulin GA, Harvey-Jones E, O'Sullivan DE, Booth CM, Sullivan R and Aggarwal A, BMJ, 2020, 371, m4087. [PubMed: 33148535]
5. Dobosz P and Dzieciatkowski T, Front Immunol, 2019, 10, 2965. [PubMed: 31921205]
6. Neek M, Kim TI and Wang SW, Nanomedicine, 2019, 15, 164–174. [PubMed: 30291897]
7. Jacob JB, Jacob MK and Parajuli P, Adv Pharmacol, 2021,91, 111–139. [PubMed: 34099106]
8. Gulubova M, Open Access Maced J Med Sci, 2019, 7, 3324–3340. [PubMed: 31949539]
9. Colonna M, Trinchieri G and Liu YJ, Nat Immunol, 2004, 5, 1219–1226. [PubMed: 15549123]
10. Whiteside TL and Odoux C, Cancer Immunol Immunother, 2004, 53, 240–248. [PubMed: 14685779]
11. Shortman K and Heath WR, Immunol Rev, 2010, 234, 18–31. [PubMed: 20193009]
12. Wang Y, Xiang Y, Xin VW, Wang XW, Peng XC, Liu XQ, Wang D, Li N, Cheng JT, Lyv YN, Cui SZ, Ma Z, Zhang Q and Xin HW, J Hematol Oncol, 2020, 13, 107. [PubMed: 32746880]
13. Chen H, Tan J, Li X, Li H, Wu W, Wu Y, Zhang J and Gu L, Oncol Lett, 2021, 21, 90. [PubMed: 33376523]
14. Skold AE, Mathan TSM, van Beek JJP, Florez-Grau G, van den Beukel MD, Sittig SP, Wimmers F, Bakdash G, Schreibelt G and de Vries IJM, Cancer Immunol Immunother, 2018, 67, 1425–1436. [PubMed: 30019146]
15. Fu C, Peng P, Loschko J, Feng L, Pham P, Cui W, Lee KP, Krug AB and Jiang A, Proc Natl Acad Sci U S A, 2020, 117, 23730–23741. [PubMed: 32879009]

16. Molino NM, Anderson AK, Nelson EL and Wang SW, ACS Nano, 2013, 7, 9743–9752. [PubMed: 24090491]
17. Molino NM, Neek M, Tucker JA, Nelson EL and Wang SW, ACS Biomater Sci Eng, 2017, 3, 496–501. [PubMed: 28989957]
18. Molino NM, Neek M, Tucker JA, Nelson EL and Wang SW, Biomaterials, 2016, 86, 83–91. [PubMed: 26894870]
19. Neek M, Tucker JA, Kim TI, Molino NM, Nelson EL and Wang SW, Biomaterials, 2018, 156, 194–203. [PubMed: 29202325]
20. Neek M, Tucker JA, Butkovich N, Nelson EL and Wang SW, Advanced Therapeutics, 2020, 3.
21. Milne JL, Wu X, Borgnia MJ, Lengyel JS, Brooks BR, Shi D, Perham RN and Subramaniam S, J Biol Chem, 2006, 281, 4364–4370. [PubMed: 16308322]
22. Bachmann MF and Jennings GT, Nat Rev Immunol, 2010, 10, 787–796. [PubMed: 20948547]
23. Nguyen B and Tolia NH, NPJ Vaccines, 2021,6, 70. [PubMed: 33986287]
24. Dalmau M, Lim S, Chen HC, Ruiz C and Wang SW, Biotechnol Bioeng, 2008, 101, 654–664. [PubMed: 18814295]
25. Dalmau M, Lim S and Wang SW, Nano Lett, 2009, 9, 160–166. [PubMed: 19113890]
26. Dalmau M, Lim S and Wang SW, Biomacromolecules, 2009, 10, 3199–3206. [PubMed: 19874026]
27. Ren D, Dalmau M, Randall A, Shindel MM, Baldi P and Wang SW, Adv Funct Mater, 2012, 22, 3170–3180. [PubMed: 23526705]
28. Ren D, Kratz F and Wang SW, Biochem Eng J, 2014, 89, 33–41. [PubMed: 25018664]
29. Ren D, Kratz F and Wang SW, Small, 2011,7, 1051–1060. [PubMed: 21456086]
30. Pettersen EF, Goddard TD, Huang CC, Meng EC, Couch GS, Croll TI, Morris JH and Ferrin TE, Protein Sci, 2021,30, 70–82. [PubMed: 32881101]
31. Zhang Y, Lin Z, Wan Y, Cai H, Deng L and Li R, Front Immunol, 2019, 10, 2472. [PubMed: 31749795]
32. Foged C, Arigita C, Sundblad A, Jiskoot W, Storm G and Frokjaer S, Vaccine, 2004, 22, 1903–1913. [PubMed: 15121302]
33. Hanlon DJ, Aldo PB, Devine L, Alvero AB, Engberg AK, Edelson R and Mor G, Am J Reprod Immunol, 2011,65, 597–609. [PubMed: 21241402]
34. Ye Y, Gaugler B, Mohty M and Malard F, Clin Transl Immunology, 2020, 9, e1139. [PubMed: 32489664]
35. Orsini G, Legitimo A, Failli A, Massei F, Biver P and Consolini R, Int Immunol, 2012, 24, 347–356. [PubMed: 22345276]
36. Xu Y, Zhan Y, Lew AM, Naik SH and Kershaw MH, J Immunol, 2007, 179, 7577–7584. [PubMed: 18025203]
37. Villadangos JA and Young L, Immunity, 2008, 29, 352–361. [PubMed: 18799143]
38. Lou Y, Liu C, Kim GJ, Liu YJ, Hwu P and Wang G, J Immunol, 2007, 178, 1534–1541. [PubMed: 17237402]
39. Ohto U, Ishida H, Shibata T, Sato R, Miyake K and Shimizu T, Immunity, 2018, 48, 649–658 e644. [PubMed: 29625894]
40. Maeda K and Akira S, Immunity, 2016, 45, 705–707. [PubMed: 27760331]
41. Dalod M, Chelbi R, Malissen B and Lawrence T, EMBO J, 2014, 33, 1104–1116. [PubMed: 24737868]
42. Edwards AD, Diebold SS, Slack EM, Tomizawa H, Hemmi H, Kaisho T, Akira S and Reis e Sousa C, Eur J Immunol, 2003, 33, 827–833. [PubMed: 12672047]
43. Hesse C, Kollenda S, Rotan O, Pastille E, Adamczyk A, Wenzek C, Hansen W, Epple M, Buer J, Westendorf AM and Knuschke T, Mol Cancer Ther, 2019, 18, 1069–1080. [PubMed: 30962317]
44. Ilyinskii PO, Roy CJ, O'Neil CP, Browning EA, Pittet LA, Altreuter DH, Alexis F, Tonti E, Shi J, Basto PA, Iannacone M, Radovic-Moreno AF, Langer RS, Farokhzad OC, von Andrian UH, Johnston LP and Kishimoto TK, Vaccine, 2014, 32, 2882–2895. [PubMed: 24593999]
45. Shirota H, Tross D and Klinman DM, Vaccines (Basel), 2015, 3, 390–407. [PubMed: 26343193]

46. Chen W, Jiang M, Yu W, Xu Z, Liu X, Jia Q, Guan X and Zhang W, Int J Nanomedicine, 2021, 16, 5281–5299. [PubMed: 34385817]
47. Butkovich N, Li E, Ramirez A, Burkhardt AM and Wang SW, Wiley Interdiscip Rev Nanomed Nanobiotechnol, 2021, 13, e1681. [PubMed: 33164326]
48. Ballas ZK, Krieg AM, Warren T, Rasmussen W, Davis HL, Waldschmidt M and Weiner GJ, J Immunol, 2001, 167, 4878–4886. [PubMed: 11673492]
49. Halperin SA, Dobson S, McNeil S, Langley JM, Smith B, McCall-Sani R, Levitt D, Nest GV, Gennevois D and Eiden JJ, Vaccine, 2006, 24, 20–26. [PubMed: 16198027]
50. Harper KB, From obscurity to a Nobel Prize nomination: Houston scientists acclaimed for their patent-free COVID-19 vaccine, https://www.texastribune.org/2022/02/10/corbevax-texas-coronavirus-vaccine/, (accessed May, 2022).
51. Campbell JD, Methods Mol Biol, 2017, 1494, 15–27. [PubMed: 27718183]
52. Meier A, Alter G, Frahm N, Sidhu H, Li B, Bagchi A, Teigen N, Streeck H, Stellbrink HJ, Hellman J, van Lunzen J and Altfeld M, J Virol, 2007, 81,8180–8191. [PubMed: 17507480]
53. Heil F, Hemmi H, Hochrein H, Ampenberger F, Kirschning C, Akira S, Lipford G, Wagner H and Bauer S, Science, 2004, 303, 1526–1529. [PubMed: 14976262]
54. Iwamoto N, Butler DCD, Svrzikapa N, Mohapatra S, Zlatev I, Sah DWY, Meena S. M. Standley, Lu G, Apponi LH, Frank-Kamenetsky M, Zhang JJ, Vargeese C and Verdine GL, Nat Biotechnol, 2017, 35, 845–851. [PubMed: 28829437]
55. Siegal FP, Kadowaki N, Shodell M, Fitzgerald-Bocarsly PA, Shah K, Ho S, Antonenko S and Liu YJ, Science, 1999, 284, 1835–1837. [PubMed: 10364556]
56. Gilliet M, Boonstra A, Paturel C, Antonenko S, Xu XL, Trinchieri G, O'Garra A and Liu YJ, J Exp Med, 2002, 195, 953–958. [PubMed: 11927638]
57. Angelov GS, Tomkowiak M, Marcais A, Leverrier Y and Marvel J, J Immunol, 2005, 175, 189–195. [PubMed: 15972647]
58. Guo X, Zhou Y, Wu T, Zhu X, Lai W and Wu L, J Immunol Methods, 2016, 432, 24–29. [PubMed: 26876301]
59. Zhang W, An EK, Hwang J and Jin JO, Front Immunol, 2021, 12, 727161. [PubMed: 34603298]
60. Li Z, Ju X, Silveira PA, Abadir E, Hsu WH, Hart DNJ and Clark GJ, Front Immunol, 2019, 10, 1312. [PubMed: 31231400]
61. Nuhn L, Vanparijs N, De Beuckelaer A, Lybaert L, Verstraete G, Deswarte K, Lienenklaus S, Shukla NM, Salyer ACD, Lambrecht BN, Grooten J, David SA, De Koker S and De Geest BG, P Natl Acad Sci USA, 2016, 113, 8098–8103.
62. Wan D, Que H, Chen L, Lan T, Hong W, He C, Yang J, Wei Y and Wei X, Nano Lett, 2021, 21, 7960–7969. [PubMed: 34533963]
63. Collier MA, Junkins RD, Gallovic MD, Johnson BM, Johnson MM, Macintyre AN, Sempowski GD, Bachelder EM, Ting JP and Ainslie KM, Mol Pharm, 2018, 15, 4933–4946. [PubMed: 30281314]
64. Seya T, Akazawa T, Tsujita T and Matsumoto M, Evid Based Complement Alternat Med, 2006, 3, 31–38; discussion 133-137. [PubMed: 16550221]
65. Sugiyama T, Hoshino K, Saito M, Yano T, Sasaki I, Yamazaki C, Akira S and Kaisho T, International Immunology, 2008, 20, 1–9. [PubMed: 17981792]
66. Kato H, Takeuchi O, Sato S, Yoneyama M, Yamamoto M, Matsui K, Uematsu S, Jung A, Kawai T, Ishii KJ, Yamaguchi O, Otsu K, Tsujimura T, Koh CS, Reis e Sousa C, Matsuura Y, Fujita T and Akira S, Nature, 2006, 441, 101–105. [PubMed: 16625202]
67. Kushwah R and Hu J, J Immunol, 2010, 185, 795–802. [PubMed: 20601611]
68. Volpi C, Fallarino F, Pallotta MT, Bianchi R, Vacca C, Belladonna ML, Orabona C, De Luca A, Boon L, Romani L, Grohmann U and Puccetti P, Nat Commun, 2013, 4, 1852. [PubMed: 23673637]
69. Takagi H, Arimura K, Uto T, Fukaya T, Nakamura T, Choijookhuu N, Hishikawa Y and Sato K, Sci Rep, 2016, 6, 24477. [PubMed: 27075414]
70. Jegalian AG, Facchetti F and Jaffe ES, Adv Anat Pathol, 2009, 16, 392–404. [PubMed: 19851130]

71. Ho NI, Huis In ‘t Veld LGM, Raaijmakers TK and Adema GJ, Front Immunol, 2018, 9, 2874. [PubMed: 30619259]
72. Monia BP, Johnston JF, Sasmor H and Cummins LL, J Biol Chem, 1996, 271, 14533–14540. [PubMed: 8662854]
73. Houseley J and Tollervey D, Cell, 2009, 136, 763–776. [PubMed: 19239894]
74. Bao M and Liu YJ, Protein Cell, 2013, 4, 40–52. [PubMed: 23132256]
75. Guiducci C, Ott G, Chan JH, Damon E, Calacsan C, Matray T, Lee KD, Coffman RL and Barrat FJ, J Exp Med, 2006, 203, 1999–2008. [PubMed: 16864658]
76. Cella M, Jarrossay D, Facchetti F, Alebardi O, Nakajima H, Lanzavecchia A and Colonna M, Nat Med, 1999, 5, 919–923. [PubMed: 10426316]
77. Reizis B, Immunity, 2019, 50, 37–50. [PubMed: 30650380]
78. Abbas A, Vu Manh TP, Valente M, Collinet N, Attaf N, Dong C, Naciri K, Chelbi R, Brelurut G, Cervera-Marzal I, Rauwel B, Davignon JL, Bessou G, Thomas-Chollier M, Thieffry D, Villani AC, Milpied P, Dalod M and Tomasello E, Nat Immunol, 2020, 21, 983–997. [PubMed: 32690951]
79. Josephs SF, Ichim TE, Prince SM, Kesari S, Marincola FM, Escobedo AR and Jafri A, J Transl Med, 2018, 16.
80. Duramad O, Fearon KL, Chan JH, Kanzler H, Marshall JD, Coffman RL and Barrat FJ, Blood, 2003, 102, 4487–4492. [PubMed: 12946990]
81. Geginat J, Larghi P, Paroni M, Nizzoli G, Penatti A, Pagani M, Gagliani N, Meroni P, Abrignani S and Flavell RA, Cytokine Growth Factor Rev, 2016, 30, 87–93. [PubMed: 26980675]
82. Gee K, Guzzo C, Che Mat NF, Ma W and Kumar A, Inflamm Allergy Drug Targets, 2009, 8, 40–52. [PubMed: 19275692]
83. Mueller SN, European Journal of Immunology, 2017, 47, 1798–1801. [PubMed: 28845904]
84. Maynard SK, Marshall JD, MacGill RS, Yu L, Cann JA, Cheng LI, McCarthy MP, Cayatte C and Robbins SH, BMC Cancer, 2019, 19, 540. [PubMed: 31170937]
85. Luchner M, Reinke S and Milicic A, Pharmaceutics, 2021, 13.
86. Rodell CB, Arlauckas SP, Cuccarese MF, Garris CS, Li R, Ahmed MS, Kohler RH, Pittet MJ and Weissleder R, Nat Biomed Eng, 2018, 2, 578–588. [PubMed: 31015631]
87. Narusawa M, Inoue H, Sakamoto C, Matsumura Y, Takahashi A, Inoue T, Watanabe A, Miyamoto S, Miura Y, Hijikata Y, Tanaka Y, Inoue M, Takayama K, Okazaki T, Hasegawa M, Nakanishi Y and Tani K, Cancer Immunol Res, 2014, 2, 568–580. [PubMed: 24830413]
88. Bhardwaj N, et al. Cancer J, 2010, DOI: 10.1097/PPO.0b013e3181eaca65.
89. Krug A, Towarowski A, Britsch S, Rothenfusser S, Hornung V, Bals R, Giese T, Engelmann H, Endres S, Krieg AM and Hartmann G, European Journal of Immunology, 2001, 31, 3026–3037. [PubMed: 11592079]

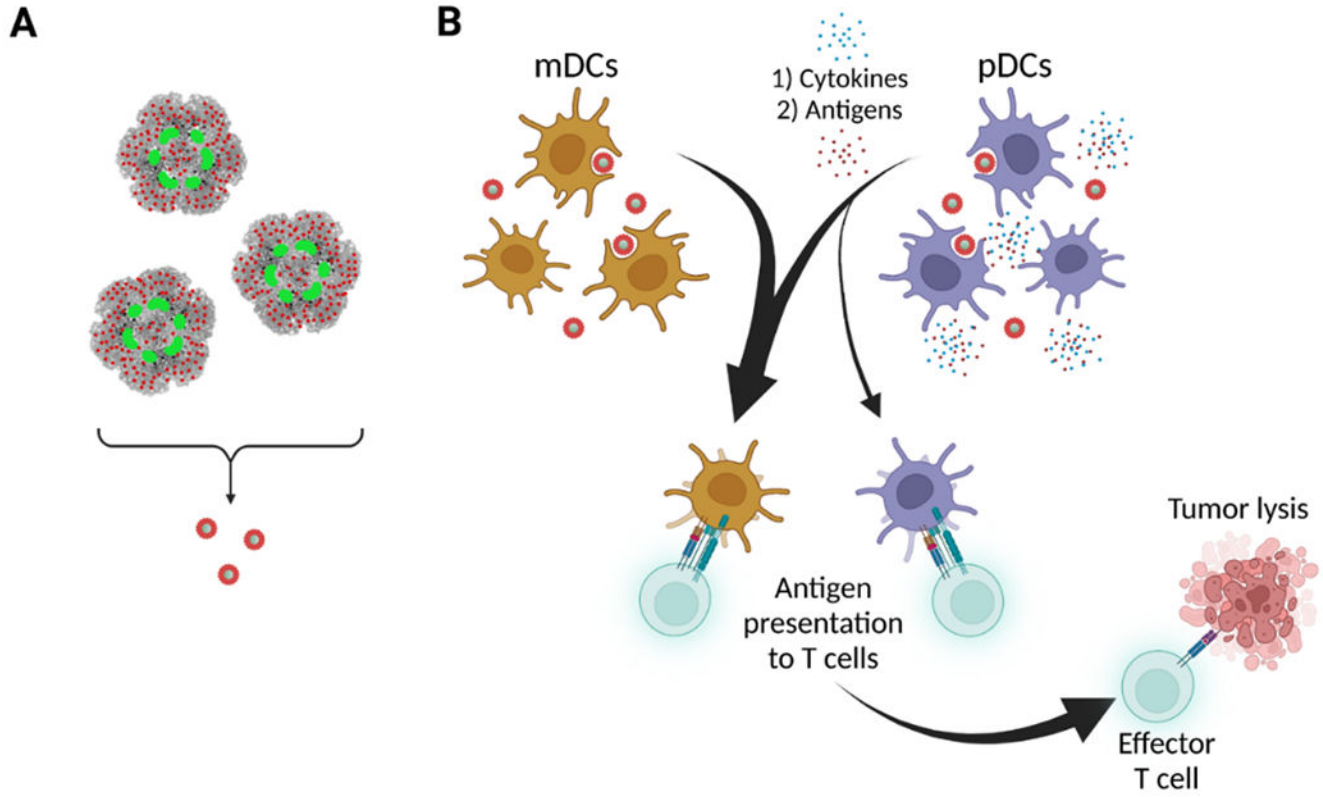

Figure 1. Proposed responses of dendritic cells to protein nanoparticle cancer vaccines.

A) E2 nanoparticle vaccines, which are represented in panel B as red circles. E2 structure (gray) was generated in ChimeraX using Protein Data Bank ID code 1b5s (E2).[30] Conjugated onto E2 are antigen (red) on the particle surface and adjuvant (green) in the interior of the particle. E2 nanoparticles are ~27 nm in diameter. **B)** Schematic of proposed mDC and pDC responses to nanoparticle cancer vaccines. In response to vaccine, mDCs and to a lesser extent pDCs may directly activate T cells, which can recognize and eliminate tumor cells. Plasmacytoid DCs may aid mDCs in this process through the transfer of cytokines and antigens. Represented are mDCs (orange cells), pDCs (purple cells), vaccine (red circles), cytokines (blue dots), antigens (red dots), T cells (turquoise cells), and lysed tumor cells (pink).

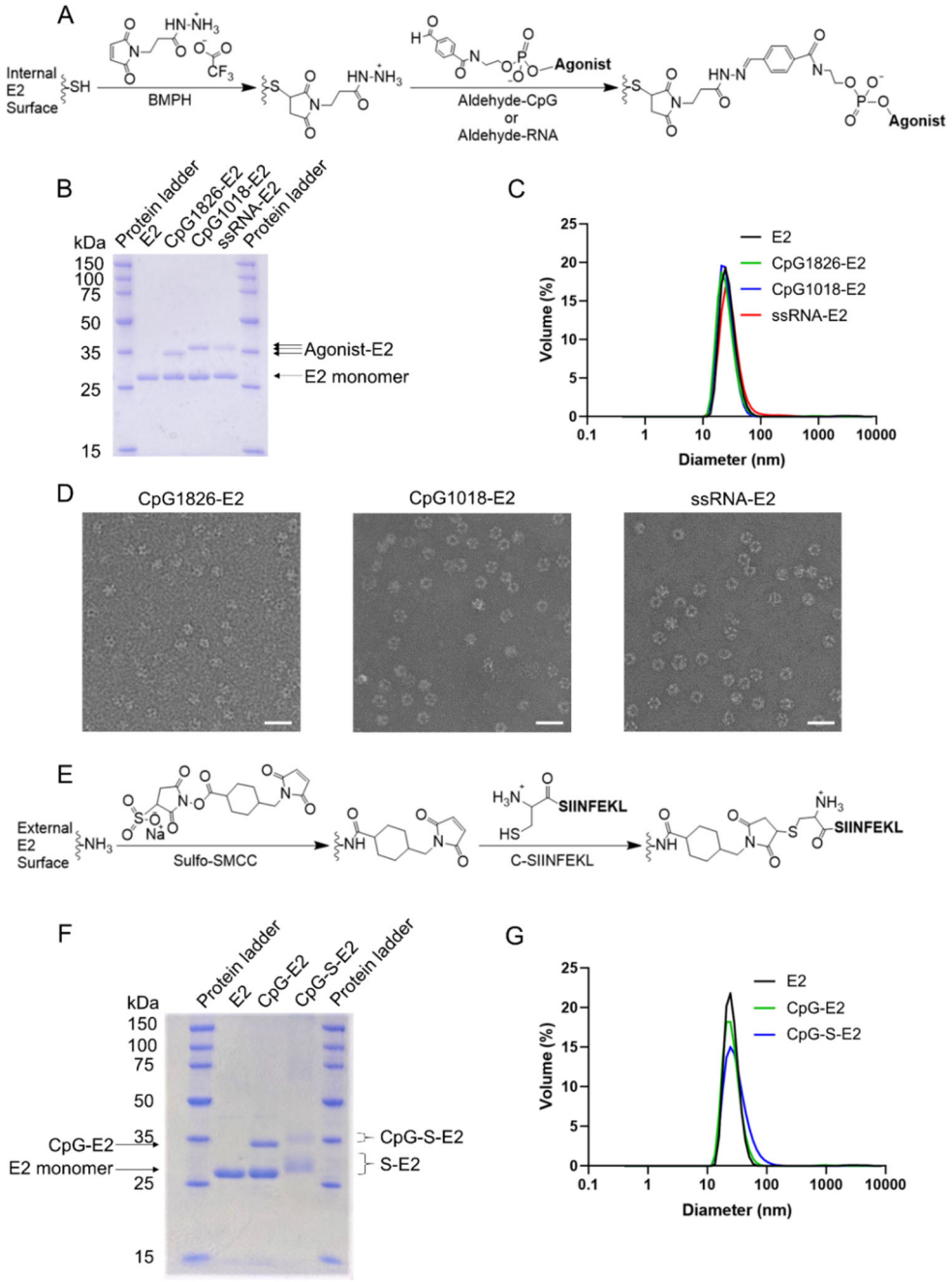

Figure 2. Adjuvant- and antigen-conjugated nanoparticles.

A) Reaction scheme for the conjugation of CpG1826, CpG1018, or ssRNA adjuvants to the interior cysteines of E2 (D381C) nanoparticles. **B)** SDS-PAGE of nanoparticles encapsulating TLR agonist. Lanes: (1,6) molecular weight ladder; (2) E2; (3) CpG1826-E2; (4) CpG1018-E2; (5) ssRNA-E2. Construct bands at ~35 kDa confirm conjugation. **C)** Representative hydrodynamic diameter measurements of E2 encapsulating TLR agonists and E2 control. **D)** Representative TEM images of CpG1826-E2, CpG1018-E2, and ssRNA-E2. Scale bars = 50 nm. **E)** Reaction scheme for the conjugation of SIINFEKL to the exterior

lysines of E2 nanoparticles. **F)** SDS-PAGE of complete E2 vaccine formulation or reaction intermediates. Lanes: (1,5) molecular weight ladder; (2) E2; (3) CpG-E2, (4) CpG-S-E2. **G)** Representative hydrodynamic diameter measurements of E2, CpG-E2, or CpG-S-E2. *CpG: CpG1826. S: SIINFEKL.*

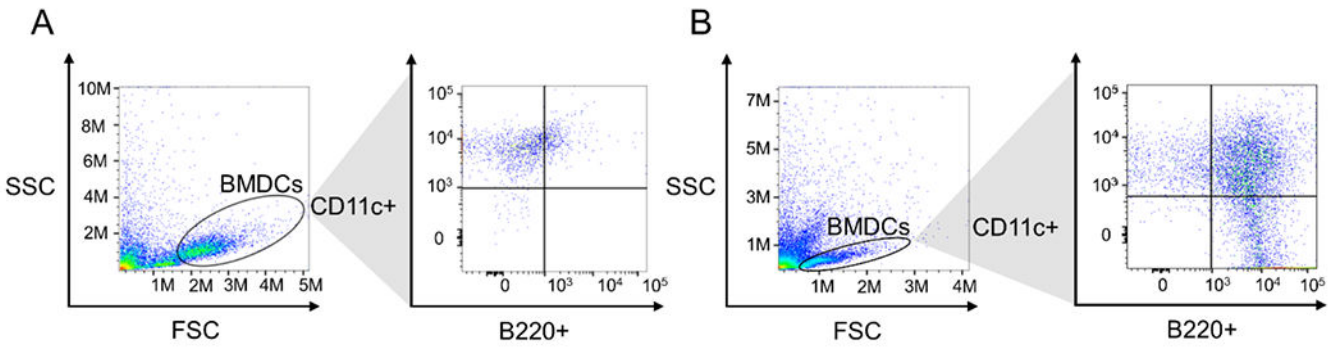

Figure 3. Evaluation of mDCs and pDCs.

Gating scheme for bone-marrow-derived **A)** mDCs and **B)** pDCs. BMDCs were first gated based on size (left panel), and then for CD11c and B220 (right panel). Subsets are phenotypically defined as $CD11c^{high}$ $B220^{-}$ mDCs and $CD11c^{low}$ $B220^{+}$ pDCs *SSC: side scatter. FSC: forward scatter.*

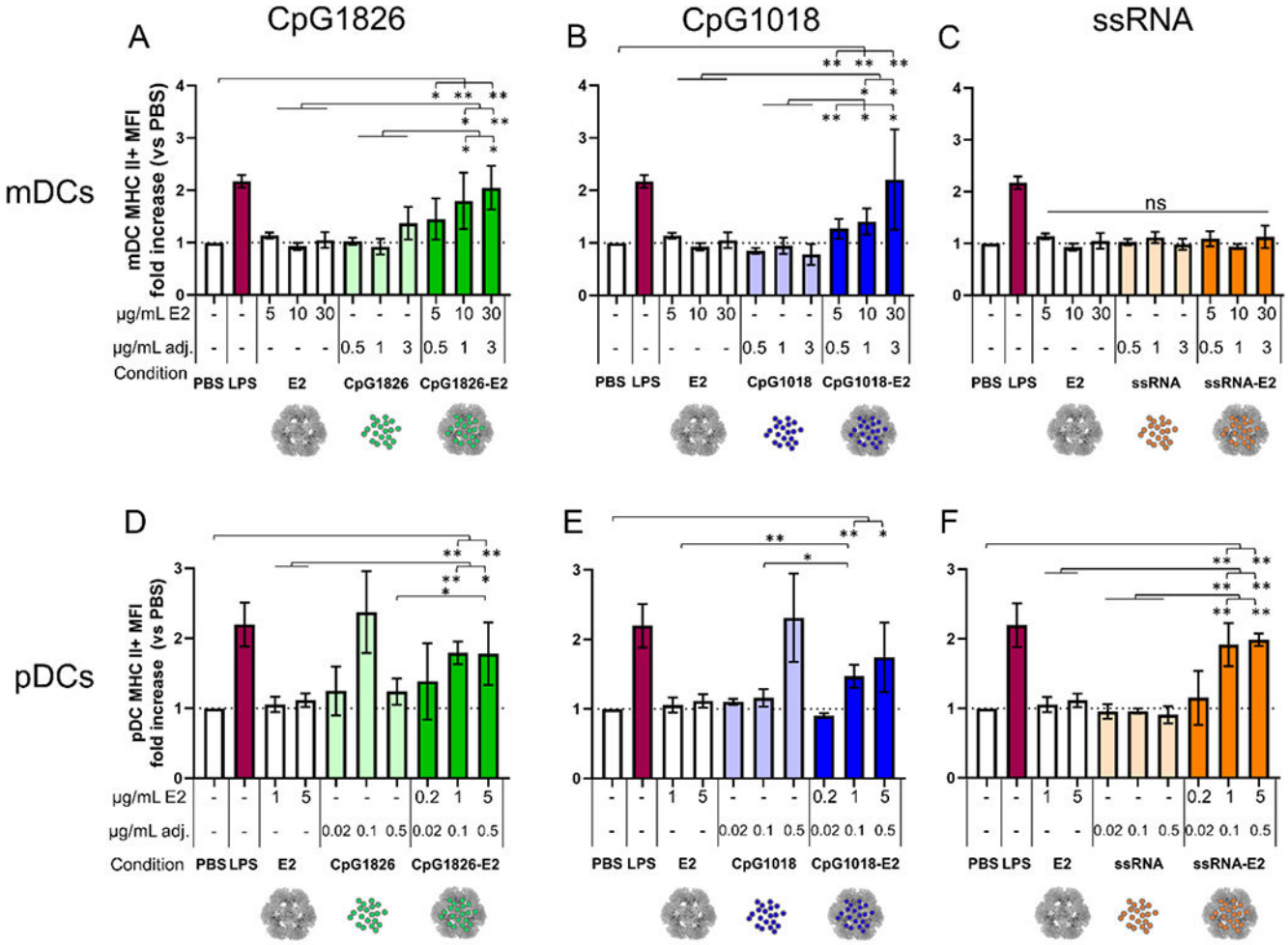

Figure 4. MHC II response of mDCs and pDCs to encapsulated TLR agonists.

Myeloid DC **(A-C)** or plasmacytoid DC **(D-F)** MHC II+ MFI fold increase versus PBS control. For each condition or formulation, corresponding concentrations of E2 and adjuvant are displayed. White bars are PBS- and E2-only controls. Red bars indicate 100 ng/mL LPS (mDC positive control) or 200 ng/mL LPS (pDC positive control). Green, blue, and orange bars correspond to free (light bars) or encapsulated (dark bars) CpG1826, CpG1018, or ssRNA, respectively. **A)** MHC II expression of mDCs incubated with PBS, LPS, E2, and CpG1826 controls or CpG1826-E2. **B)** MHC II expression of mDCs incubated with CpG1018-E2 or control. **C)** MHC II expression of mDCs incubated with ssRNA-E2 or control. **D)** MHC II expression of pDCs incubated with CpG1826-E2 or control. **E)** MHC II expression of pDCs incubated with CpG1018-E2 or control. **F)** MHC II expression of pDCs incubated with ssRNA-E2 or control. *Mean ± SEM. Statistics: 1-way ANOVA, Bonferroni's test. ≥3 independent biological replicates, 2-3 technical replicates per independent biological replicate. Adj: adjuvant. *p ≤ 0.05, **p ≤ 0.01.* Experimental procedure is outlined in Figure SI-1.

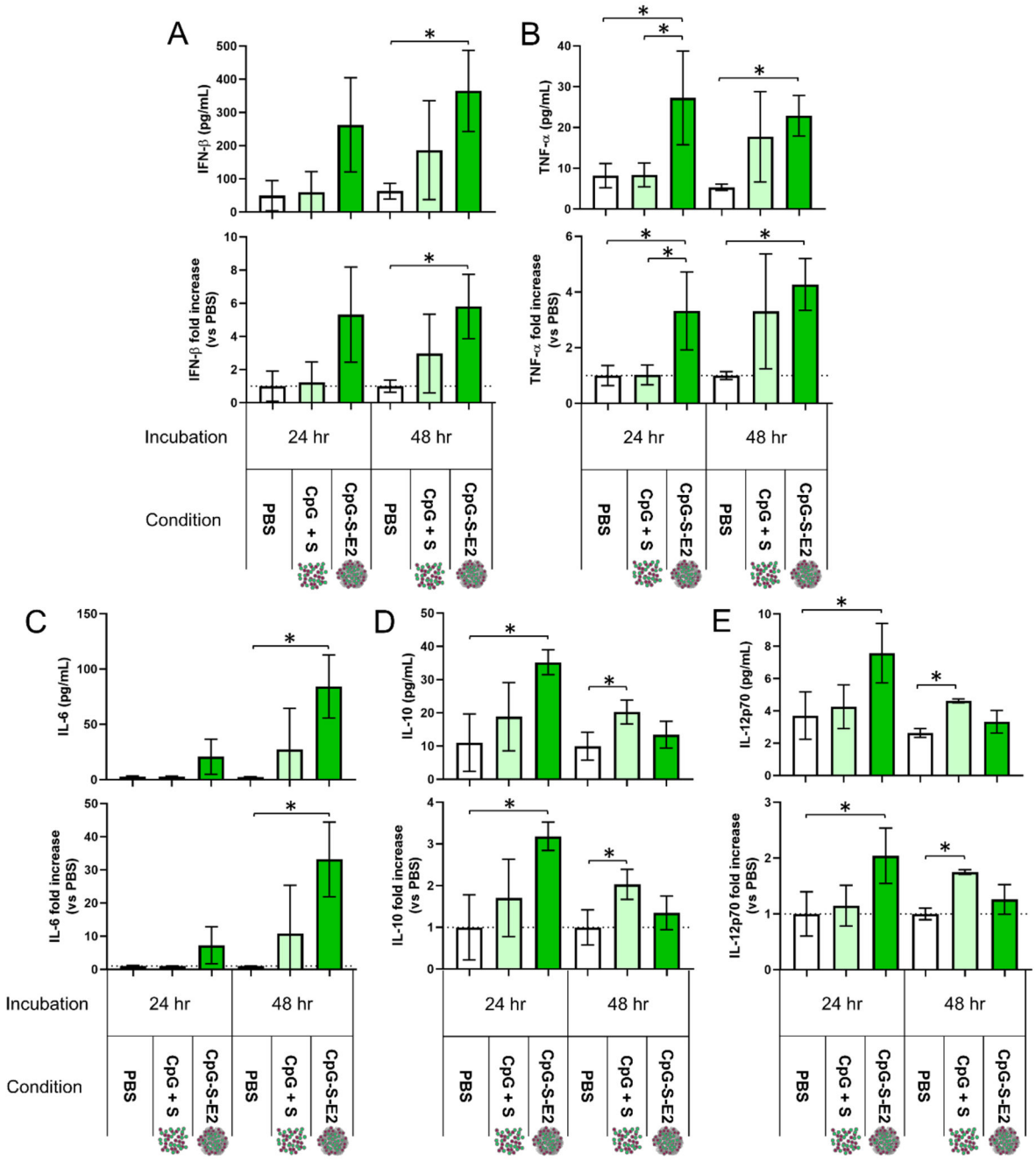

Figure 5. Plasmacytoid DCs secrete an array of cytokines in response to incubation with vaccine.

Displayed are concentrations of cytokines (top graph of each set) and fold increase in cytokine concentration relative to PBS negative control (bottom graph of each set), secreted from pDCs after incubation with vaccine or control. For 24 hr or 48 hr incubation periods, pDC secretions of **A)** IFN-β, **B)** TNF-α, **C)** IL-6, **D)** IL-10, and **E)** IL-12p70 were determined by LegendPlex™ assay. Incubation conditions included PBS, 0.1 μg/mL CpG1826 with 0.1 μg/mL SIINFEKL (CpG + S), or CpG-S-E2 containing 0.1 μg/mL CpG1826 with 0.1 μg/mL SIINFEKL. *Mean ± SEM. Statistics: 1-way ANOVA,*

*Bonferroni's test. 3 independent biological replicates, 2 technical replicates per biological replicate. CpG: CpG1826. S: SIINFEKL. *p ≤ 0.05.*

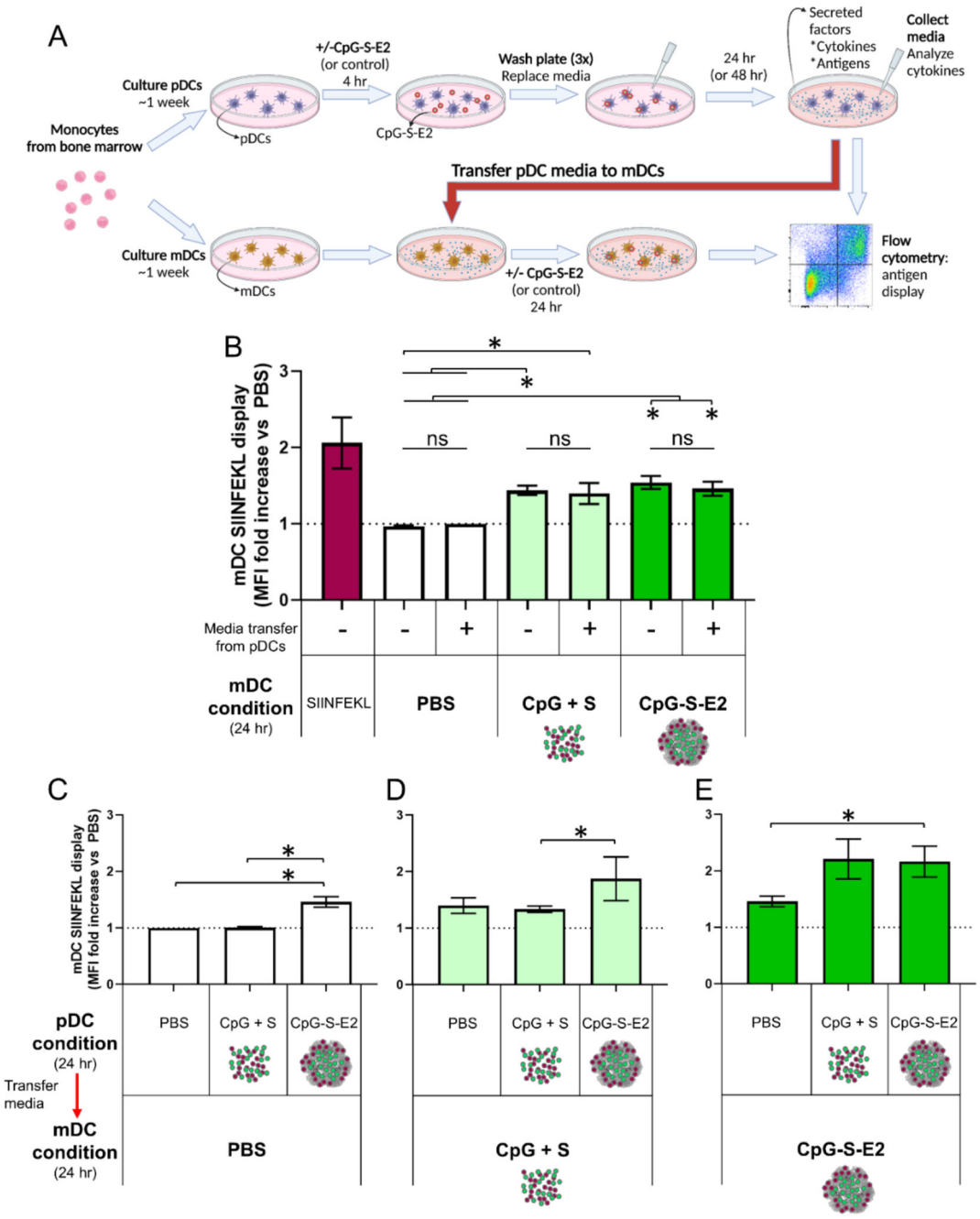

Figure 6. Plasmacytoid DCs aid mDCs to display antigen.

A) Schematic for pDC supernatant transfer studies. For incubation steps, mDCs or pDCs were given 1 μg/mL CpG-S-E2 vaccine or controls (PBS negative control, 2 μg/mL SIINFEKL positive control, or 0.1 μg/mL CpG1826 with 0.1 μg/mL SIINFEKL). **B)** Myeloid DC SIINFEKL display with or without media transfer from pDCs that were incubated with PBS for 24 hr starting on Day 8. **(C-E)** Myeloid DC SIINFEKL display following supernatant transfer protocol for mDCs or pDCs incubated with **C)** PBS, **D)** 0.1 μg/mL CpG1826 with 0.1 μg/mL SIINFEKL, and **E)** 1 μg/mL CpG-S-E2 (containing 0.1

μg/mL CpG1826 with 0.1 μg/mL SIINFEKL) for 24 hr starting on Day 9 (mDCs) or Day 8 (pDCs). Shown is display fold increase in antigen display versus that of mDCs incubated with PBS. *Mean ± SEM. Statistics: 1-way ANOVA, Bonferroni's test. 3 independent biological replicates, 2-3 technical replicates per biological replicate. CpG: CpG1826. S: SIINFEKL. *p ≤ 0.05*.